iScience, Volume *23*

Supplemental Information

A Spatially Resolved Dark- versus Light-Zone Microenvironment Signature Subdivides Germinal Center-Related Aggressive B Cell Lymphomas

Claudio Tripodo, Federica Zanardi, Fabio Iannelli, Saveria Mazzara, Mariella Vegliante, Gaia Morello, Arianna Di Napoli, Alessandro Mangogna, Fabio Facchetti, Sabina Sangaletti, Claudia Chiodoni, Alison VanShoiack, Anand D. Jeyasekharan, Stefano Casola, Mario P. Colombo, Maurilio Ponzoni, and Stefano A. Pileri

Supplemental Information

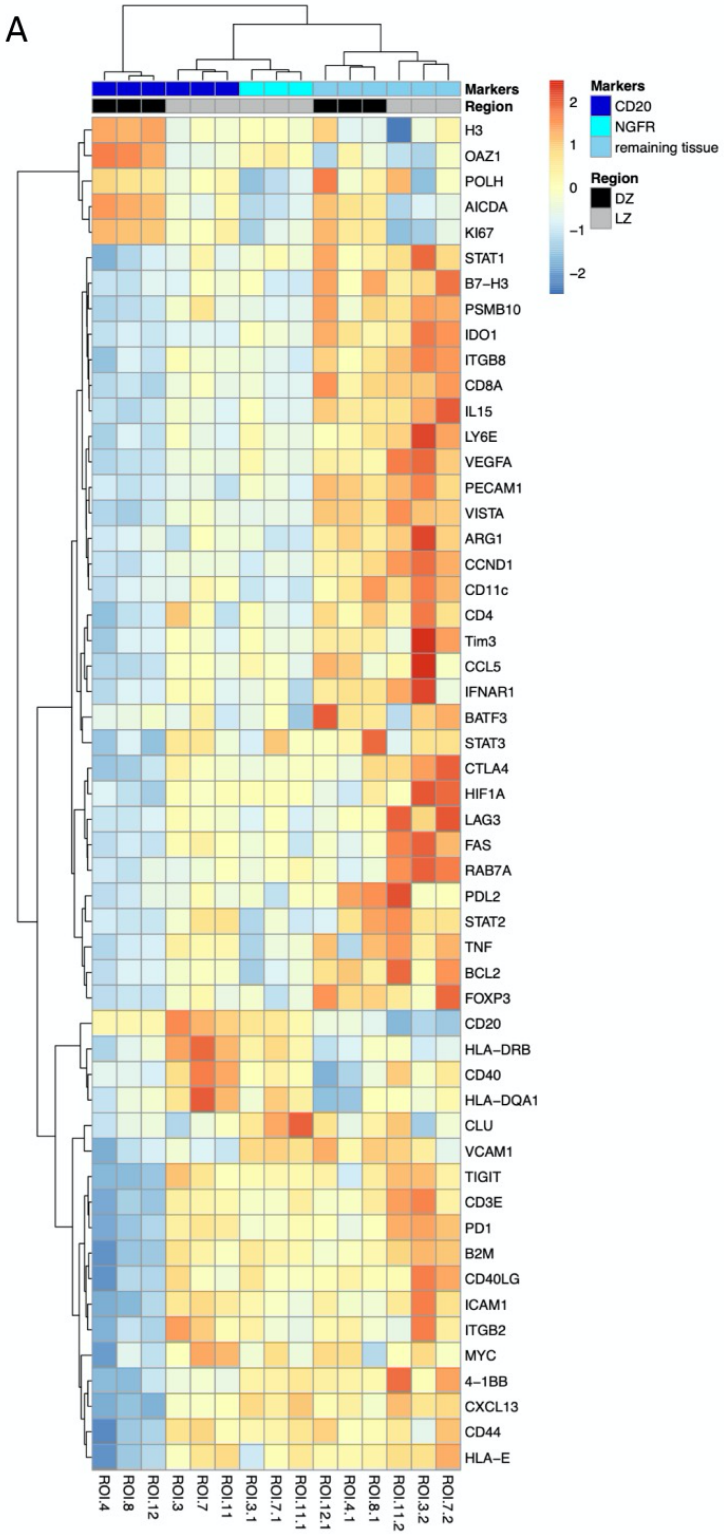

Figure S1, Related to Figure 1. Clustering of DZ and LZ ROIs according to the 53 differential genes assessed in different ROI masks as shown in Figure 1C. **A)** Clustering of the 53 genes discriminating DZ and LZ reveals different contribution of B-cell (CD20) FDC (NGFR) and remaining tissue ROI sub-compartments.

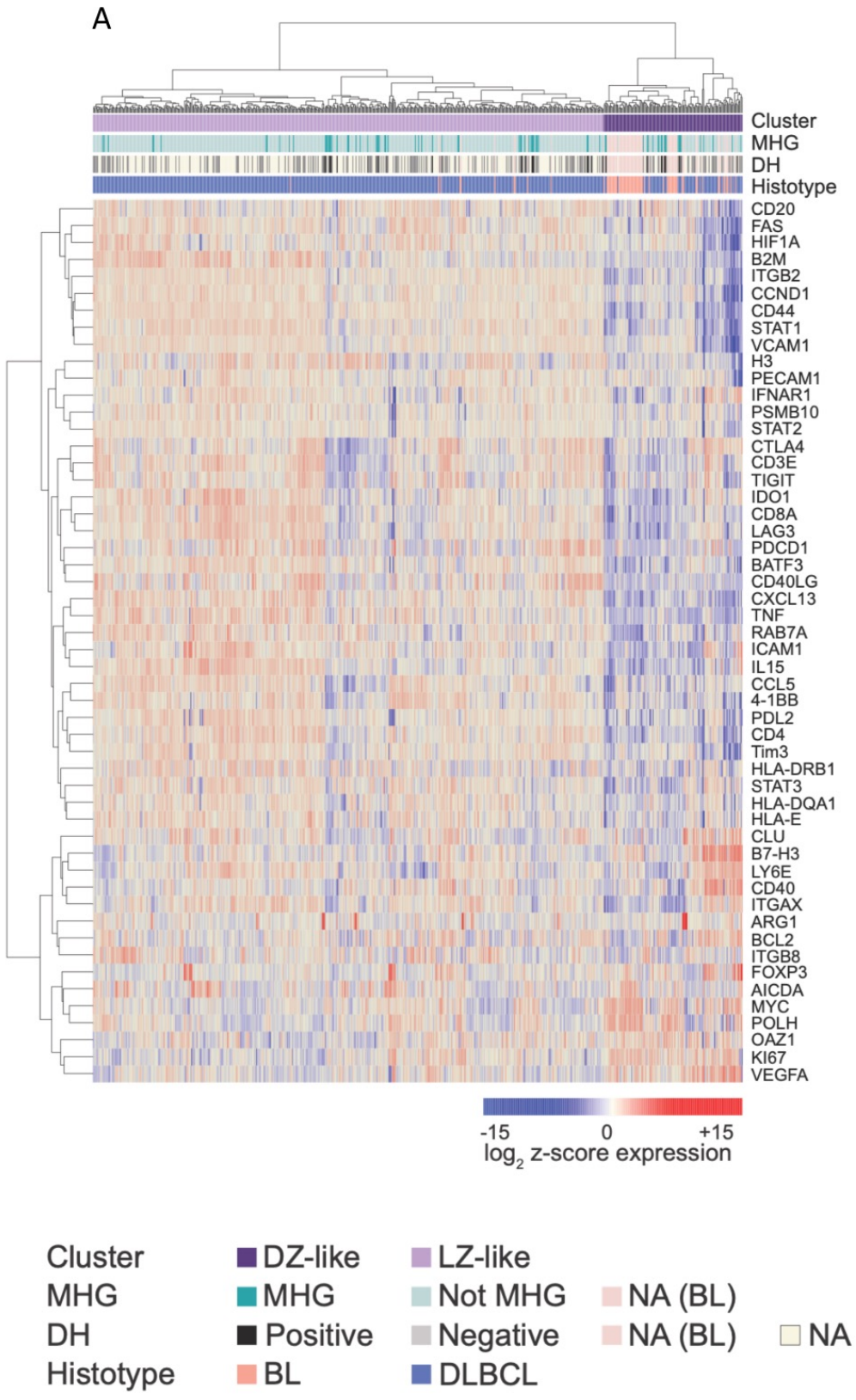

Figure S2, Related to Figure 4. Unsupervised hierarchical clustering of Sha's dataset (GSE117556) extended to Burkitt Lymphoma (BL) cases, according to the 53 genes DZ/LZ spatial signature. **A)** The heatmap representing z-score normalized values of the 53 genes reveals that the majority of BL (56 out of 70, 80%) are classified in the DZ-like cluster with molecular high-grade GC-related DLBCL samples.

A

Figure S3, Related to Figure 5. Analysis of the overlap between the 25 genes DZ/LZ stromal signature and Lenz's stromal signatures (Lenz et al., 2008). **A)** Only one gene, *CLU*, was shared with the Stromal-1 and one gene, *PECAM1*, with the Stromal-2 signature, indicating that a different level of heterogeneity is probed through the 25 genes DZ/LZ stromal microenvironment signature.

Transparent Methods

To investigate the immune and stromal composition of two spatially-resolved GC microenvironments, namely the DZ and LZ, multiplexed wide field immunofluorescence (IF) analysis was combined to ROIs definition and segmentation, and in situ mRNA analysis to screen four-micrometer thick tissue sections from formalin-fixed and paraffin-embedded reactive lymph nodes using a GeoMx Digital Spatial Profiler (DSP) (NanoString, Seattle WA) (Merritt et al., 2020). Samples were collected according to the Helsinki Declaration and the study was approved by the University of Palermo Institutional Review Board (approval number 09/2018).The following antibodies were adopted for 4-plex IF tissue imaging: mouse anti-human CD20 (L26 Novocastra, Leica Biosystems), mouse anti-human CD271 (NGFR, MRQ-21 Cell Marque), mouse anti-human SMA (ASM-1 Novocastra, Leica Biosystems). Syto83 was used as nuclear counterstain in DSP IF-based ROI selection while DAPI was adopted for validation IF stainings.

For the determination of the 87-plex customized TAP Human Immuno Oncology panel, mRNA binding DNA probes (5′ to 3′ 35- to 50-nt target-complementary sequences) conjugated with UV photocleavable indexing oligos were hybridized to the tissue as previously reported (Merritt et al., 2020). The UV photocleavable probes were released from each ROI according to custom masks for UV illumination and digitally counted using the NanoString nCounter Analysis System. For nCounter data analysis, digital counts from barcodes corresponding to mRNA probes were normalized to internal spike-in controls (ERCC). Moreover, a set of six internal housekeeping genes was included in the TAP Human Immuno Oncology panel to control for system variation including ROI size and cellularity (Decalf et al., 2019; Merritt et al., 2020). Seven negative control probes were adopted to evaluate and filter ROIs with a high degree on non-specific binding (none identified in this experiment). Normalized gene expression data relative to the ROIs analyzed in this study are reported in Table S4. Unsupervised hierarchical clustering of the ROIs was performed on the normalized counts using the pheatmap function of the homonymous R package with default parameters. Genes differentially expressed between LZ and DZ ROIs were identified by applying an empirical Bayes test using the Limma R package.

CD20, CD44, CD54, H3, Ki-67, and MYC expression in GC DZ and LZ of the lymph nodes profiled by DSP was validated at the protein level using double- or triple marker immunostainings (Figure 2). Double- and triple-marker immunostainings on reactive lymph nodes were performed as follows: four micrometers-thick sections from formalin fixed and paraffin-embedded lymph node biopsies were put onto positively-charged slides, deparaffinized and rehydrated. Sections underwent heath-induced antigen retrieval using Novocastra Epitope Retrieval Solution pH9 (Leica Biosystems). Slides underwent sequential rounds of incubation at room temperature for 1h with the following primary antibodies: mouse anti-human CD20 (1:100, clone L26,

Novocastra, Leica Biosystems), rabbit anti-human Ki-67 (1:1000, Abcam), rabbit anti-human c-MYC (1:500, clone Y69, Abcam), goat anti-human Histone-H3 (1:150, Abcam), mouse anti-human CD44 (1:40, clone DF1485, Novocastra, Leica Biosystems), mouse anti-human CD54 (1:30, clone 23G12, Novocastra, Leica Biosystems). Primary antibodies binding was revealed by the use of specific secondary antibodies conjugated with either horseradish peroxidase (HRP) or fluorophores (Alexa 488, Alexa 568, Invitrogen; Opal 520, Opal 620, Akoya Biosciences). 3,3'-diaminobenzidine (DAB) was used as chromogenic substrate for HRP. Slides were analyzed under a Zeiss Axioscope-A1 microscope equipped with bright field fluorescence module (Zeiss). Microphotographs were collected with a Zeiss Axiocam 503 Color digital camera using the Zen 2.0 imaging software (Zeiss).

The spatial DZ/LZ signatures were tested in the following independent transcriptomic datasets: GSE38697; GSE117556. For both datasets we used normalized expression data provided by the Authors. To further validate the 53 genes DZ/LZ spatial signature in *bona fide* DZ-derived aggressive lymphomas, we integrated the 70 Burkitt Lymphoma samples (GSE69051) from Sha et al., with the DLBCL samples (GSE117556). Raw data from these samples were processed with the Limma R package to generate normalized values applying a quantile normalization. Where multiple probes represented the same gene, the gene expression was summarized with the maximum value. After performing z-score normalization, hierarchical clustering based on the spatially-resolved DZ/LZ 53 genes signature and/or on the 25 stromal genes signature was applied to identify clusters reflecting GC heterogeneity. Hierarchical clustering analysis was performed using Ward.D2 and Euclidean distance. The rand-index measure was used to quantify the similarity of two clustering results. For survival analysis, we used Kaplan-Meier with log-rank tests to estimate overall survival between the identified clusters. Differences in patient characteristics were analyzed using the χ^2 test; a p-value <0.05 was set as the threshold for significance. To visualize the overlapped genes between the different signatures we applied Euler R package (https://cran.r-project.org/package=eulerr). All statistical analyses were performed using R statistical software package (v 3.6.0) (http://www.R-project.org).

Supplementary References

Decalf, J., Albert, M.L., and Ziai, J. (2019). New tools for pathology: a user's review of a highly multiplexed method for in situ analysis of protein and RNA expression in tissue. J Pathol *247*, 650-661.

Lenz, G., Wright, G., Dave, S.S., Xiao, W., Powell, J., Zhao, H., Xu, W., Tan, B., Goldschmidt, N., Iqbal, J.*, et al.* (2008). Stromal gene signatures in large-B-cell lymphomas. N Engl J Med *359*, 2313-2323.

Merritt, C.R., Ong, G.T., Church, S.E., Barker, K., Danaher, P., Geiss, G., Hoang, M., Jung, J., Liang, Y., McKay-Fleisch, J.*, et al.* (2020). Multiplex digital spatial profiling of proteins and RNA in fixed tissue. Nat Biotechnol *38*, 586-599.